Metamorphic History and Geochemistry of a Low-grade Amphibolite in the Kaserer Formation (Marginal Bündner Schiefer of the Western Tauern Window, the Eastern Alps)

by *W. Frisch**

Abstract

A low-grade amphibolite, probably an original dolerite sill, in the Lower Cretaceous Kaserer Formation has been investigated. Microprobe analyses on relictic amphiboles of an early metamorphic event show that the later regional metamorphism, which is of the low-grade type, has a lower P/T-regime than the early one. Amphibole, plagioclase, epidote, and chlorite demonstrate that the low-grade metamorphism was prograde and that the grade increases from N(E) towards S(W).

The chemical composition of the amphibolite is largely that of an ocean-floor basalt (MORB), which has been spilitized to some extent and partly contaminated with potassium. For geological reasons the depositional environment of the Kaserer Formation is considered a small basin on the thinned slope on the south margin of the Middle Penninic microcontinent.

Keywords: Amphibolite, low-grade metamorphism, amphiboles, geochemistry, Bündner Schiefer, Tauern Window, Eastern Alps.

Zusammenfassung

Aus der unterkretazischen Kaserer Formation des Tauernfensters wurde ein Epidot-Amphibolit, vermutlich ein ursprünglicher Dolerit-Lagergang, untersucht. Mikrosondenanalysen an reliktischen Amphibolen einer frühen metamorphen Phase zeigen, dass die spätere epizonale Regionalmetamorphose ein niedrigeres P/T-Regime aufweist als die frühe Metamorphose. Amphibol, Plagioklas, Epidot und Chlorit lassen erkennen, dass diese niedriggradige Metamorphose prograd ablief, und dass der Metamorphosegrad von N(E) nach S(W) zunimmt.

Die chemische Zusammensetzung des Amphibolits ist weitgehend die eines Ozeanboden-Basaltes (MORB), der bis zu einem gewissen Grad spilitisiert und teilweise mit Kalium verunreinigt wurde. Aus geologischen Gründen wird der Ablagerungsbereich der Kaserer Formation in einem kleinen Becken am ausgedünnten Kontinentalabhang an der Südseite des mittelpenninischen Mikrokontinents gesehen.

* Institut für Geologie und Paläontologie, Sigwartstr. 10, D-7400 Tübingen.

1. Introduction

The Kaserer Formation (Thiele, 1970; Frisch, 1980) represents a clastic series in the western part of the Tauern window. With regard to its position above at least partly Upper Jurassic Hochstegen marble, a Lower to Middle Cretaceous age is assigned to it. A basin on the continental slope plunging from the Zentralgneiss complex in the north towards the oceanic South Penninic basin in the south is supposed to be the area of deposition for the rocks of the Kaserer Formation. Thus, it represents a marginal facies of the Bündner Schiefer, which were deposited in the basin and on its flanks.

In the lowest part of the approximately 200 m thick series the sediments are contaminated by basic tuffs (chlorite schists with abundant epidote). In the higher part of the sequence, a medium-grained low-grade (epidote) amphibolite can be pursued for some distance. This member is the topic of the present paper. From the Tuxer Joch it has been described as amphibolite by Sander (1911) and Bleser (1934). A more recent description is given by Höck (1969). A short characterization of the Kaserer Formation is given by Frisch (1980).

2. Occurrence and petrography of the amphibolite

The occurrence of the amphibolite in the area Brenner pass Tuxer Joch is shown in Fig. 1. The disruptions are in part due to lack of outcrops, in part probably of tectonic origin, and not primary. The eastern end of the horizon is unknown.

The amphibolite is a rock of mesoscopically medium-grained habit. Despite cleavage and preferred orientation of minerals the rock has preserved its original massive appearance. Under the microscope the large grains are disintegrated into recrystallized aggregates of much smaller size. Only large amphibole crystals may take the place of the original pyroxene phenocrysts, and (albitized) relict plagioclase is rare. The probably holocrystalline and relatively coarse-grained original rock is considered a doleritic sill which intruded into a shallow level but possibly was an effusive basalt flow.

The thickness of the amphibolite decreases towards the SW: 1–2 m near Brenner pass, 2–5 m in Valser Tal. At Napf Spitze it thickens tectonically to about 100 m. Near Tuxer Joch the thickness is less than 20 m. Therefore, the outcrops in the northeast are considered to be closer to the feeder than those in the southwest.

The mineral assemblage is granoblastic and is adapted to the medium-to high-T part of low-grade metamorphism. It is characterized by the paragenesis: actinolite / actinolitic hornblende / magnesio-hornblende + chlorite + albite / oligoclase + epidote + sphene + calcite + iron oxides. Zoning of amphibole,

Fig. 1 Sketch map showing the low-grade (epidote) amphibolite in the Kaserer Formation, and sample localities (1–7).

plagioclase, and epidote attests to changes in the P,T conditions during metamorphism. Zircon, apatite, quartz, and biotite are present in some samples. Two samples contain white mica which is arranged in traces along s-planes.

2.1 THE AMPHIBOLES

Generally, the amphiboles form granular aggregates that may mimic the shape of the magmatic pyroxenes. Small intergranular crystals are also abundant.

A series of microprobe analyses was done on three samples (2, 4, 6) (table 1, Fig. 2). Actinolite, actinolitic hornblende, and magnesio-hornblende are pres-

Table 1 Microprobe analyses of amphiboles of samples 2, 4 and 6, and cation concentrations calculated on the basis of 23 oxygens. Fe^{+3} calculated with $(Y + Z) = 13$. A = actinolite, AH = actinolitic hornblende, MH = magnesio-hornblende.

Sample	2	2	2	2	2	2	4	4	4	4	4	4	4
SiO_2	54.99	51.50	51.35	49.03	47.56	46.46	54.49	53.10	51.79	45.15	45.06	44.19	43.69
TiO_2	0.10	0.02	0.16	0.14	0.30	0.29	0.01	--	0.04	0.25	0.32	0.46	0.28
Al_2O_3	1.79	4.70	5.68	7.77	10.65	11.70	2.03	3.14	4.17	12.87	13.43	14.09	14.69
FeO	10.14	10.94	12.37	12.33	13.14	12.13	10.97	11.56	11.85	14.42	14.18	14.80	14.17
MgO	16.57	15.61	14.34	13.14	11.91	11.86	16.42	16.20	15.49	10.34	10.01	9.40	9.77
MnO	0.32	0.20	0.40	0.38	0.30	0.16	0.06	0.34	0.20	0.36	0.21	0.33	0.32
CaO	13.44	12.35	12.81	12.78	11.81	11.45	13.41	13.02	12.50	11.77	11.76	11.50	11.62
Na_2O	0.19	0.52	0.50	0.77	1.04	1.41	0.07	0.36	0.44	1.58	1.53	1.60	1.67
K_2O	0.02	0.19	0.08	0.17	0.19	0.25	0.04	0.11	0.20	0.20	0.30	0.33	0.38
Si	7.84	7.51	7.41	7.19	6.96	6.85	7.80	7.62	7.53	6.68	6.66	6.57	6.49
Al	0.16	0.49	0.59	0.81	1.04	1.15	0.20	0.38	0.47	1.32	1.34	1.43	1.51
Al	0.15	0.32	0.38	0.53	0.79	0.89	0.14	0.15	0.25	0.92	1.00	1.03	1.06
Ti	0.01	--	0.02	0.02	0.04	0.04	--	--	0.01	0.03	0.04	0.05	0.04
Fe	1.21	1.33	1.49	1.52	1.61	1.50	1.32	1.39	1.44	1.79	1.75	1.84	1.76
Mg	3.52	3.39	3.09	2.87	2.59	2.61	3.50	3.47	3.35	2.29	2.20	2.08	2.16
Mn	0.04	0.03	0.05	0.04	0.04	0.02	0.01	0.04	0.03	0.04	0.03	0.04	0.04
Ca	2.06	1.93	1.98	2.01	1.86	1.81	2.05	2.00	1.95	1.87	1.86	1.83	1.85
Na	--	0.07	0.02	--	0.14	0.19	--	--	0.05	0.13	0.14	0.17	0.15
Na	0.05	0.07	0.12	0.21	0.16	0.22	0.02	0.10	0.07	0.31	0.30	0.29	0.33
K	--	0.04	0.02	0.04	0.04	0.05	--	0.02	0.03	0.04	0.05	0.07	0.07
Y	4.93	5.07	5.03	4.98	5.07	5.06	4.97	5.05	5.08	5.07	5.02	5.04	5.06
X	2.06	2.00	2.00	2.01	2.00	2.00	2.05	2.00	2.00	2.00	2.00	2.00	2.00
A	0.05	0.11	0.14	0.25	0.20	0.27	0.02	0.12	0.10	0.35	0.35	0.36	0.40
Fe^{+3}	--	0.24	0.10	--	0.23	0.18	--	0.18	0.27	0.23	0.06	0.17	0.22
	A	A	AH	AH	MH	MH	A	A	A	MH	MH	MH	MH

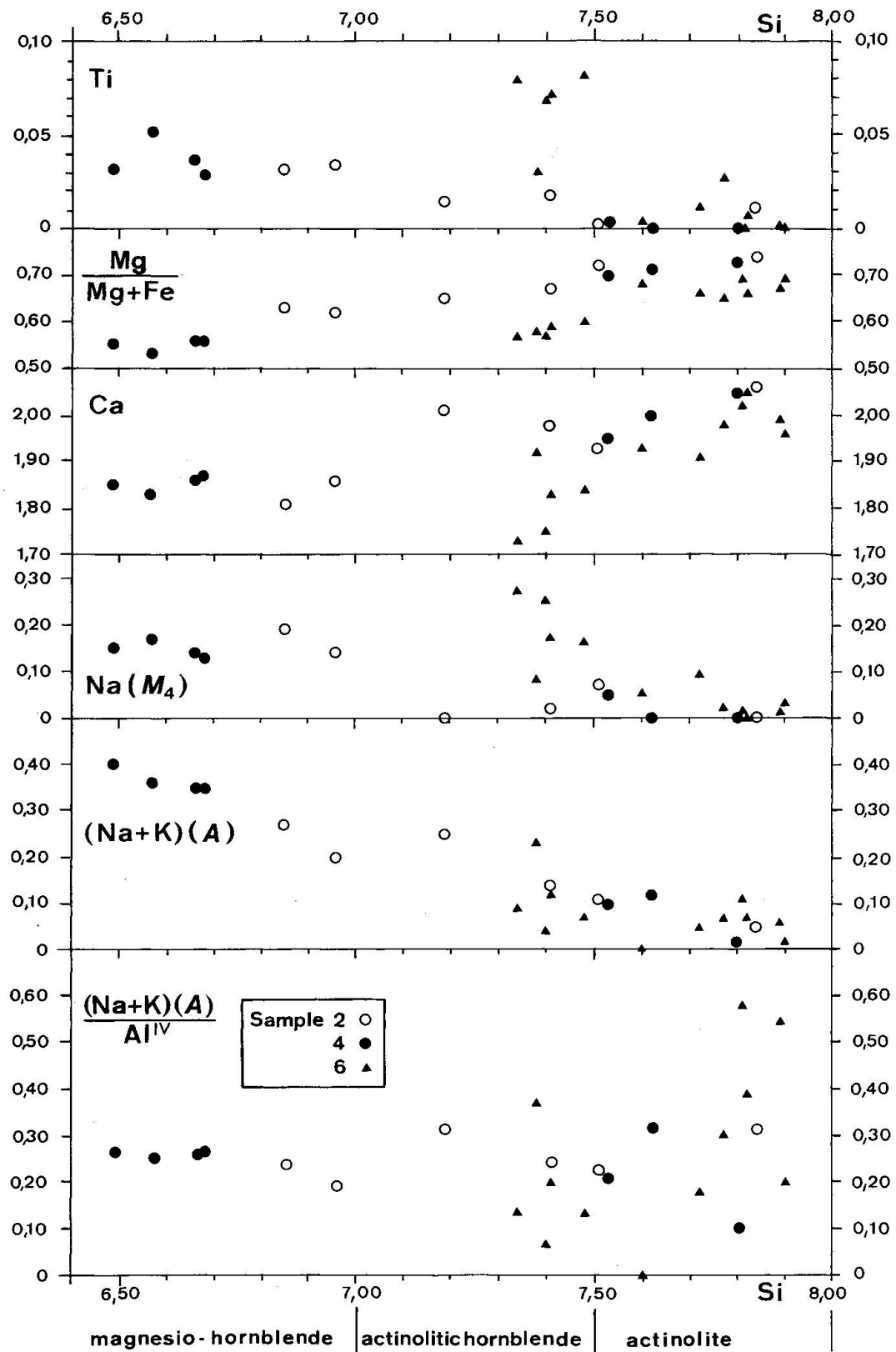| Sample	6	6	6	6	6	6	6	6	6	6	6	6
SiO_2	55.07	54.25	54.46	53.39	53.88	53.56	51.18	50.78	51.29	49.69	49.67	49.64
TiO_2	--	0.01	0.06	--	0.21	0.10	0.04	0.73	0.65	0.61	0.27	0.71
Al_2O_3	1.39	1.37	1.53	2.86	1.95	2.45	4.07	4.69	5.67	5.49	4.83	5.85
FeO	12.68	13.23	13.69	11.39	14.19	13.76	12.12	15.09	15.33	15.89	16.35	16.33
MgO	15.52	14.75	14.87	14.60	14.67	14.99	14.45	12.69	12.55	12.01	12.51	12.05
MnO	0.20	0.30	0.27	0.01	0.30	0.55	0.34	0.41	0.43	0.53	0.37	0.59
CaO	12.75	12.79	13.30	12.88	12.87	12.34	12.12	11.64	11.83	10.91	12.03	10.91
Na_2O	0.12	0.23	0.17	0.29	0.32	0.46	0.16	0.80	0.93	0.96	1.02	1.15
K_2O	0.06	--	0.07	0.14	--	0.09	0.01	0.03	0.19	0.13	0.09	0.10
Si	7.90	7.89	7.82	7.81	7.77	7.72	7.60	7.48	7.41	7.40	7.38	7.34
Al	0.10	0.11	0.18	0.19	0.23	0.28	0.40	0.52	0.59	0.60	0.62	0.66
Al	0.14	0.12	0.08	0.30	0.10	0.14	0.31	0.29	0.38	0.37	0.22	0.35
Ti	--	--	0.01	--	0.03	0.01	0.01	0.08	0.07	0.07	0.03	0.08
Fe	1.52	1.61	1.65	1.40	1.71	1.66	1.51	1.86	1.85	1.98	2.04	2.02
Mg	3.32	3.20	3.19	3.18	3.15	3.22	3.20	2.79	2.70	2.67	2.77	2.66
Mn	0.03	0.03	0.03	--	0.03	0.07	0.04	0.05	0.05	0.06	0.04	0.07
Ca	1.96	1.99	2.05	2.02	1.98	1.91	1.93	1.84	1.83	1.75	1.92	1.73
Na	0.03	0.01	--	--	0.02	0.09	0.05	0.16	0.17	0.25	0.08	0.27
Na	--	0.06	0.05	0.09	0.07	0.03	--	0.07	0.09	0.02	0.21	0.07
K	0.02	--	0.02	0.02	--	0.02	--	--	0.03	0.02	0.02	0.02
Y	5.01	4.96	4.96	4.88	5.02	5.10	5.07	5.07	5.05	5.15	5.10	5.18
X	1.99	2.00	2.05	2.02	2.00	2.00	1.98	2.00	2.00	2.00	2.00	2.00
A	0.02	0.06	0.07	0.11	0.07	0.05	--	0.07	0.12	0.04	0.23	0.09
Fe^{+3}	--	--	--	--	0.05	0.32	0.27	0.26	0.19	0.53	0.34	0.60
	A	A	A	A	A	A	A	AH	AH	AH	AH	AH

Fig. 2 Variation diagrams of amphibole compositions from the amphibolite in the Kaserer Formation.

ent. Because of the characteristic pleochroism of these three phases a distribution of the amphiboles could be traced for all samples:

(1) Southwestern part (Valser Tal and south of it, samples 1, 2, 4, 5, without sample 3):

(a) *actinolite:* cores of mainly large crystals, patches (nγ pale bluish green).

(b) *magnesio-hornblende:* margins of large grains and patches in centre, entire small grains,(nγ light to medium bluish green with a slight brownish tinge).

The boundaries between the two amphibole phases are, in general, narrow transition zones. Magnesio-hornblende is the younger amphibole. The chemical differences are shown in Fig. 2.

(2) Sample 7 from Tuxer Joch and sample 3 from a tectonic complication at Venn Spitze contain *actinolite* as the only amphibole.

(3) Sample 6 from Napf Spitze:

(a) *actinolitic hornblende:* broad cores of large crystals (nγ dirty olivebrown).

(b) *actinolite,* as above: rims of, and patches in, large crystals, or entire small grains.

The two amphibole phases of sample 6 are often sharply separated. Despite their small chemical differences, they contrast well in thin section. Here actinolite is the younger phase. The olive-brown actinolitic hornblende decomposes to chlorite. This is not the case with the other amphiboles, which appear to have crystallized in equilibrium with chlorite (see below).

The actinolitic hornblende in sample 1 is transitional between actinolite and magnesio-hornblende. The chemical composition of the older actinolitic hornblende in sample 6 is quite different (Fig. 2).

2.2 PLAGIOCLASE

Large, partly euhedral, marginally recrystallized single albite crystals (An 0–6; universal stage measurements) are albite- and Carlsbad-twinned and represent albitized relics of the magmatic plagioclase. Some clinozoisite filling is present, but most of it migrated into the intergranular space. Towards the northeast the portion of this plagioclase generation increases.

The recrystallized plagioclase are untwinned granoblastic crystals. In the southwest (samples 1, 2) they are oligoclase beyond the peristerite gap (2Vγ = 90° or slightly more). In the central part of the area (samples 4, 5) there is less granoblastic plagioclase, and the crystals are frequently zoned: albite cores (An 0–5) border sharply on oligoclase rims (An ca. 17–20). Samples 3 and 7 contain only albite without oligoclase rims. The size of the recrystallized plagioclase grains increases from about 0,02–0,05 mm in the NE to about 0,1–0,15 mm in the SW.

2.3 EPIDOTE

Epidote (clinozoisite-pistacite) is a prominent constituent of all Samples. It is present as partly euhedral intergranular blasts. They are zoned, the pistacite (Pi) portion decreasing from core to rim. A very narrow outer seam may again be a little Pi-richer (samples 3, 6).
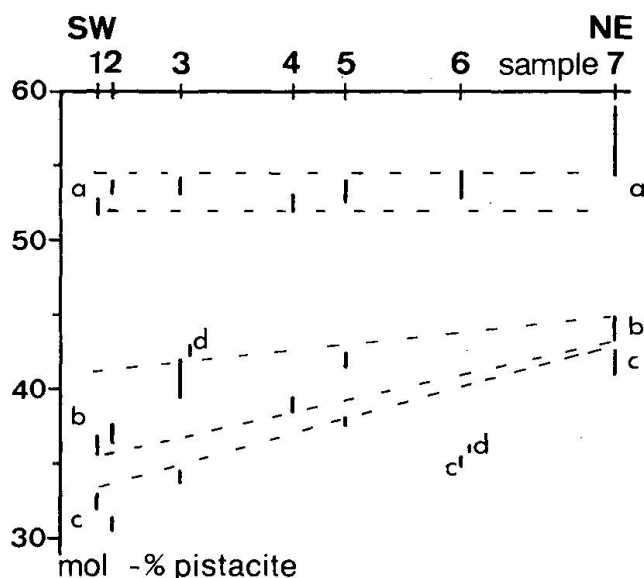

Fig. 3 Composition of zoned epidote crystals in the amphibolite. a, cores of crystals. b, broad rims. c, narrow outer rims. d, local outermost rims (retrograde). Note decrease in pistacite content of b and c in direction of increased metamorphism (dashed lines).

The compositions of the epidotes are shown in Fig. 3 (determination of birefringence with the Berek compensator; in some cases universal-stage 2V measurement, in one case microprobe analysis). The Pi-contents are uniformly 52–54 mol-% in the cores of the crystals. This coincides with the lower, Pi-poorer limit of the miscibility gap determined by RAITH (1976) for low-grade metamorphism. Only in sample 7 (Tuxer Joch) Pi was found to be up to 59% in the cores.

The broad rims are separated from the cores by a narrow transition zone. In many cases there is a narrow outer rim, again poorer in Pi. The Pi values in the outer zones of the epidotes are lower in the SW than in the NE: broad rim with Pi 36–38 (SW) to 43–45 (NE), narrow outer rim with Pi 31–33 (SW) to 41–43 (NE).

2.4 CHLORITE

The chlorite is rhipidolite in all cases. The Mg/Fe-ratio increases systematically from NE to SW (exception: sample 3). In the NE (samples 6, 7) chlorite aggregates show marginal interlayering with chlorites slightly richer in Fe.

Table 2 Microprobe analyses of chlorite of samples 2, 4 and 6, and cation concentrations calculated on the basis of 14 oxygens.

Sample	2	4	4	4	6	6
SiO_2	26.85	26.10	25.81	26.48	25.98	25.37
TiO_2	0.14	0.08	0.12	0.05	--	0.04
Al_2O_3	21.57	21.84	21.47	22.17	21.31	21.46
FeO	18.50	19.97	19.41	20.39	23.61	23.22
MgO	20.05	17.88	18.61	18.94	16.23	15.79
MnO	0.34	0.37	0.18	0.26	0.19	0.21
CaO	0.03	--	0.01	0.03	0.03	--
Na_2O	0.04	--	--	--	0.02	0.03
K_2O	--	0.02	--	--	--	0.05
Si	2.73	2.71	2.70	2.69	2.72	2.69
Al	1.27	1.29	1.30	1.31	1.28	1.31
Al	1.32	1.39	1.35	1.34	1.35	1.37
Ti	0.01	0.01	0.01	0.01	--	0.01
Fe	1.57	1.74	1.69	1.73	2.07	2.06
Mg	3.03	2.78	2.90	2.87	2.53	2.50
Mn	0.03	0.03	0.02	0.02	0.02	0.02
Ca	0.01	--	--	0.01	0.01	--
Na	0.01	--	--	--	--	--
K	--	--	--	--	--	0.01
Σ (X+Y)	5.98	5.95	5.97	5.98	5.98	5.97
$\frac{100 \; Mg}{Mg+Fe}$	66	61	63	62	55	55

Microprobe analyses were done in samples 2, 4 and 6 (table 2). The Si/Al ratio in tetrahedral position remains the same in all samples, but the Mg/Fe-ratio changes. With the help of birefringence and the assumption of a constant Si/Al-ratio, the Mg/Fe-ratio can also be determined in the other samples with good accuracy. The portion of the Mg-chlorite is about 65 mol-% in the SW and decreases to about 55 % in the NE. In the marginal iron-rich interlayers of samples 6 and 7, the Mg-chlorite portion is slightly lower than 50 %. The chlorite of sample 3 contains about 55–60 % Mg-chlorite.

3. Interpretation of mineral parageneses and metamorphic history

The investigated low-grade amphibolite permits the reconstruction of more than one phase of evolution. The igneous stage is followed by an early metamorphic event. Evidence for this early metamorphism is only based on the actinolitic hornblendes in sample 6. The main low-grade metamorphism is re-

sponsible for the present parageneses and can be divided into two stages in pro-
grade succession.

3.1 RELICT FABRICS AND MINERALS

After CIPW norm calculations the An-content of the original plagioclase
was near 50% (average 53%). Taking into account some Ca-Na exchange dur-
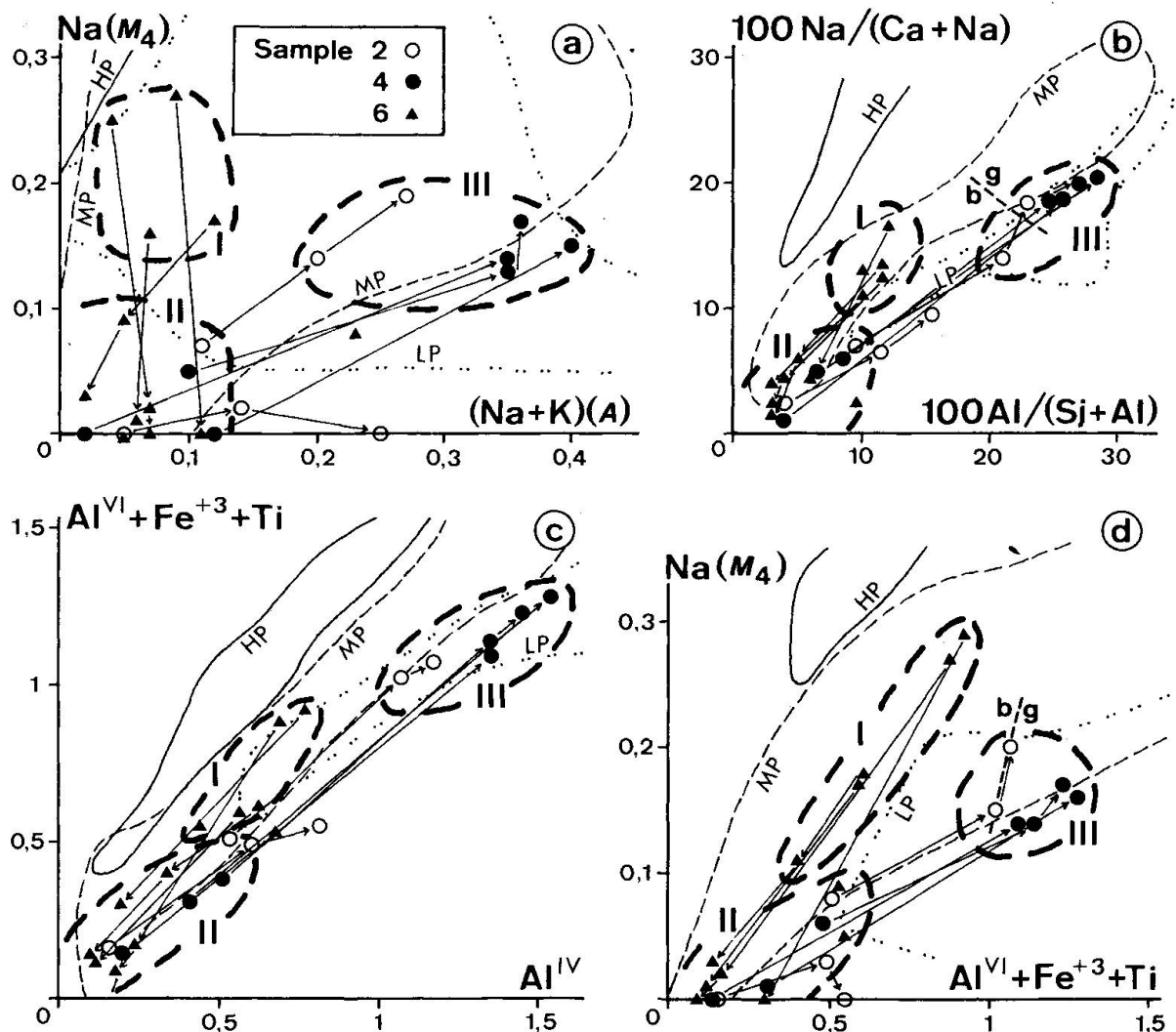ing spilitization (see below), the magmatic plagioclase certainly was a labrador-
ite.

Fig. 4 Diagrams for amphiboles after LAIRD & ALBEE (1981). Symbols as in fig. 2. Shown are the compositional
ranges of amphiboles for high-, medium-, and low-pressure areas in Vermont (HP, MP, LP), and the dividing line
between biotite and garnet zones in Vermont (b/g in diagrams b and d). Arrows point in direction of rims of crys-
tals. I, relictic amphibole of older metamorphic event with higher P/T. II, actinolites, and III, magnesio-horn-
blende of prograde main metamorphism.

Relict igneous mineral shapes (replaced by metamorphic aggregates) and structures (medium-grained fabric) have already been mentioned. Ophitic textures cannot be recognized. Relict albitized plagioclase is less scarce in the NE, where metamorphism and recrystallization were less intensive than in the SW (see below).

The early actinolitic hornblende of sample 6 has a composition deviating from the uniform trend of the other amphibole phases. In comparison to these younger amphiboles, the actinolitic hornblende of sample 6 has higher Na (M_4) and lower (Na + K) $(A)/$ Al^{IV} values (fig. 2). Both point to a *higher* (not high-) pressure regime (BROWN, 1977, resp. HIETANEN, 1974). This is confirmed by several diagrams in LAIRD & ALBEE (1981) which show a systematic change in amphibole composition with pressure regime (fig. 4). The P/T ratio is shown to be distinctly higher in the relict brownish hornblende of sample 6 than in the magnesio-hornblende equilibrated during later low-grade metamorphism. It belongs to the medium-pressure facies series of LAIRD & ALBEE, characterized by the presence of kyanite in metapelites.

3.2 LOW-GRADE METAMORPHISM

The early stage of the low-grade metamorphism is characterized by the paragenesis: actinolite + albite (An 0–6) + epidote (Pi 52–54) + chlorite (rhipidolite with about 55% Mg-chlorite) + sphene ± magnetite ± calcite. In the SW of the investigated area oligoclase may already have been stable, since the cores of the recrystallized plagioclases are oligoclase.

In the NE a later stage of the low-grade metamorphic event cannot be distinguished from the early one; there is no significant mineralogical difference between them. Only epidote shows a change in the physico-chemical conditions by its zoning.

From the Valser Tal to the south (exception: sample 3 from Venn Spitze), however, the rims of grains show a paragenesis of a somewhat higher grade: magnesio-hornblende + oligoclase (An ca. 17–20) + epidote (Pi ca. 30–40) + chlorite (60–65% Mg-chlorite) + sphene ± magnetite ± calcite.

In comparison to actinolite, magnesio-hornblende reflects a higher grade of metamorphism. This can be concluded from the increased Al^{IV}-, Al^{VI}-, Ti-, Na-, K-, and Fe/Mg-values (LAIRD, 1982, LEAKE, 1971, HIETANEN, 1974). According to the diagrams of LAIRD & ALBEE (1981), the magnesio-hornblendes cross the border from the biotite to the garnet zone (fig. 4b, d, and other diagrams not shown here). They correlate better with low-P than with medium-P amphiboles (fig. 4). The zoned amphiboles with actinolite cores and magnesio-hornblende rims reflect prograde metamorphism.
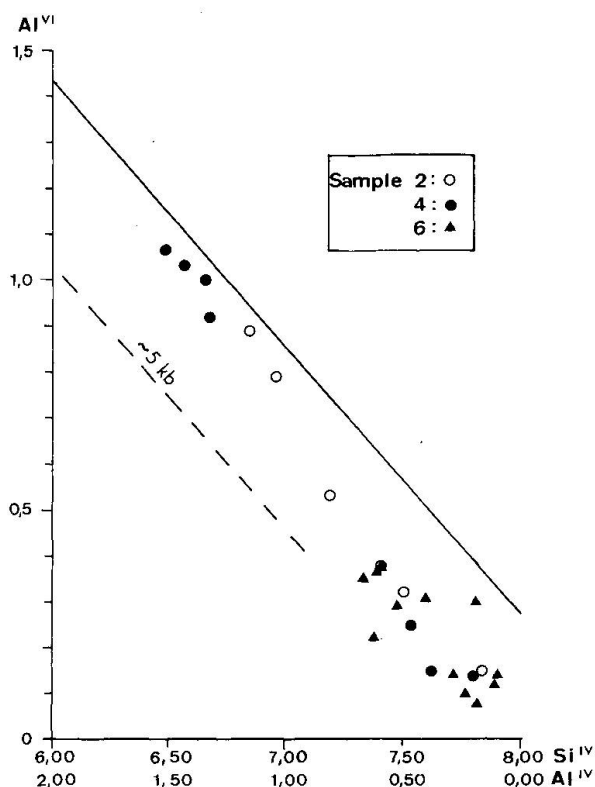
Fig. 5 Al^{VI} versus Al^{IV} diagram for the analyzed amphiboles. Full line marks the maximum possible Al^{VI} after LEAKE (1965). Amphiboles ($Al^{IV} > 1,00$) formed at pressures < 5 kb should plot below the dashed line (RAASE, 1974).

On the other hand, RAASE (1974) showed that hornblendes with Al^{VI} values close to the highest possible values (LEAKE, 1965) should indicate pressures of more than about 5 kb. The magnesio-hornblende of our samples plot in this field (fig. 5). A reliable estimate of the pressure after this diagram, however, is not possible.

After HIETANEN (1974), the relatively constant values of (Na + K) $(A)/Al^{IV}$ = 1 : 4 (0.25) for the actinolites and magnesio-hornblendes (fig. 2) point to a constant P/T-ratio during the prograde metamorphism. The large scatter field of the actinolites is due to the low (Na + K) (A) figures. HIETANEN (1974) found (Na + K) $(A)/Al^{IV}$-values of around 1 : 3 in contact aureoles, and of about 1 : 7 in kyanite-bearing sequences.

The increase of the Mg/Fe-ratio of chlorite from NE to SW corresponds to the increase in temperature in the same direction during the low-grade metamorphism. After LAIRD (1982), there is a decrease of Fe and an increase in Mg in the chlorite formula passing from greenschist to epidote-amphibolite. The slightly more iron-rich marginal parts of the chlorites in the northeastern area (samples 6, 7) reflect retrograde conditions. In these samples chlorite is in contact with K-white mica which is otherwise absent.

The increase in size and proportion of recrystallized, granoblastic plagioclase, and the increase in the An-content of plagioclase rims from NE to SW, correlate with the increase in T in the same direction during this stage. In the central part the zoned plagioclase attests to prograde evolution.

In general, with prograde metamorphism a Fe^{+3}-poorer epidote is formed (RAITH, 1976, HIETANEN, 1974). This is explained by the change of oxygen fugacity with prograde metamorphism. For the later stage of low-grade metamorphism, lower Pi-values are reached in the SW than in the NE. Epidote is also zoned in the samples from the NE where the other minerals do not allow to draw a distinction between stages of the prograde metamorphism.

3.3 GRADE OF REGIONAL METAMORPHISM

Regional metamorphism was prograde and remained in the low-grade range after WINKLER (1979). According to the mineral parageneses, temperatures remained below 500° C in the early stage (see diagrmms in WINKLER, 1979). Towards the S(W), an increase in T more than 500° C during this stage is possibly indicated by oligoclase cores of the granoblastic plagioclase which may have been in equilibrium with actinolite or actinolitic hornblende (see table 1, sample 2). This is true if the oligoclase cores formed primarily and not by re-equilibration during the second stage. In the first case, the "oligoclase-in" before "hornblende-in" would mean a rather low P/T-regime according to LAIRD & ALBEE (1981).

In a later stage, the An 17 + hornblende isograd has been surpassed in the southwestern and central parts of the investigated area. Temperatures higher than 500° C are required (WINKLER, 1979). In the NE they still remained below this limit. Beginning recrystallization of plagioclase, however, indicates temperatures not much below 500° C (VOLL, 1980).

Based on oxygen isotope data, HOERNES & FRIEDRICHSEN (1974) determined temperatures of 500°C near Tuxer Joch, and of 550°C in the Valser Tal and north of Brenner pass for the thermal peak. These isotherms have to be shifted slightly towards the south. They run unconformably towards the western margin of the Tauern window where fault scarps cause a rapid plunge of the strata.

Pressure is difficult to estimate. Data from amphiboles suggest that the P/T-ratio war relatively low during the low-grade metamorphism. According to LAIRD & ALBEE (1981), a P/T facies transitional between their low-P and medium-P series fits with the data. A pressure of about 4±0,5 kb at 500°C may be realistic.

Sample 3 deviates from the general trend: like in sample 7, temperatures remain below the An 17 + hornblende isograd. This is due to its higher tectonic (and topographic) position. The rock is strongly sheared.

The brownish amphibole relics of sample 6 indicate a higher pressure regime of this early metamorphic phase in comparison to the later low-grade metamorphism. After LAIRD & ALBEE (1981; see fig. 4) and the (Na + K) $(A)/Al^{IV}$-values (HIETANEN, 1974; see fig. 2) it crystallized under kyanite facies conditions. A pressure of more than about 4 kb at 500 °C is required (HOSCHEK, 1980 and pers. comm.). In the vicinity of the investigated area kyanite partly replaced by mica is found in metapelites (FRISCH, 1968). This kyanite may belong to the early Alpine metamorphism.

4. Geochemistry

Table 3 gives the results of chemical analyses. Changes of the primary composition may have occurred due to seawater interaction and metamorphism. As will be shown later, the chemical data suggest a slight CaO decrease and Na_2O increase due to spilitization in nearly all samples. CaO does not correlate with the modal calcite portion (8 vol-% calcite in sample 3). Calcite, together with chlorite, clearly grew at the expense of actinolite in this sample. CaO did not migrate from outside.

SiO_2 shows deviation towards lower values in samples 1, 2 (least), and 5. This becomes evident when calculated on a dry or evenly hydrated base (see figs. 6a, b). MgO is subject to major variations. K_2O is conspicuously elevated in samples 6 and 7 (mineralogically expressed in the presence of K-mica), and probably migrated from the sedimentary country rock. Rb correlates with K_2O. Among the trace elements, Ni, Sr, and, to a minor extent, Ba show variations, which are considered to be due to a certain mobility of these elements.

In the Ne'-Ol'-Q' triangle after IRVINE & BARAGAR (1971), which is not shown here, the samples fall into the "under-saturated" field within the subalkaline (= non-alkaline) series. Samples 1 and 5 deviate due to SiO_2 loss.

In figs. 6–10 a number of diagrams using major and trace elements are shown. Many of them are based on immobile or only slightly mobile elements. In almost all diagrams the samples plot in the fields of tholeiitic basalts or, more specifically, of ocean-floor basalts. Because of the high (and irregular) water + carbon dioxide contents of the samples (up to 6,6%), the element concentrations were calculated to an average water content of 1% before being plotted.

The absolute values of most elements (concentration calculated to 1% H_2O) correlate with ocean-floor basalts (see table 3). Al_2O_3 is somewhat higher and corresponds to the concentration in calc-alkaline basalts. CaO is too low, and Na_2O too high for ocean-floor basalts. The two elements show a negative correlation. This is attributed to spilitization. Most of the trace element concentrations fit well with the average values for ocean-floor basalts. FeO_{tot}, Al_2O_3 and Y correlate better with calc-alkaline basalts.

Table 3 Chemical analyses of seven samples of the amphibolite. Column 8 gives the mean values calculated with 1% water, column 9 average ocean-floor basalt, mean values from several sources (ENGEL et al., 1965, HART, 1976, PEARCE, 1976, PEARCE & CANN, 1973).

Sample	1	2	3	4	5	6	7	$\bar{x}$	OFB
SiO_2	45.89	48.46	47.39	49.13	43.97	49.37	49.53	49.03	49.61
TiO_2	1.11	1.14	1.40	1.35	1.50	1.58	1.31	1.38	1.43
Al_2O_3	18.15	17.49	17.24	17.06	17.34	17.25	16.51	17.79	16.40
Fe_2O_3	1.85	1.91	1.77	1.55	2.12	2.23	2.59		
FeO	6.69	6.63	6.08	7.39	8.63	7.13	7.21	9.16*	9.39*
MnO	0.15	0.14	0.12	0.15	0.17	0.15	0.16	0.15	0.17
MgO	8.19	8.34	5.55	7.45	9.22	6.28	6.52	7.57	7.54
CaO	10.20	9.22	9.56	8.42	9.54	9.59	9.71	9.74	11.42
Na_2O	3.20	3.54	3.63	3.92	2.53	3.05	3.46	3.43	2.77
K_2O	0.12	0.09	0.09	0.08	0.11	1.05	0.46	0.10**	0.19
P_2O_5	0.12	0.11	0.15	0.19	0.18	0.15	0.13	0.15	0.15
H_2O	2.41	2.47	3.36	2.32	3.27	2.02	1.91	(1.00)	1.02
CO_2	1.84	0.56	3.27	0.96	0.63	0.64	0.54	--	--
Sum	99.92	100.10	99.61	99.97	99.21	100.49	100.04		
V	154	168	179	174	275	221	209	203	286
Cr	238	199	280	238	244	195	298	249	294
Ni	160	177	61	167	205	53	79	132	110
Co	20	24	18	24	27	22	20	23	32
Ga	17	17	13	17	19	17	15	17	
Sc	30	30	30	32	41	37	35	35	
Rb	<10	<10	<10	<10	<10	29	13	<10	<10
Sr	346	414	241	218	364	176	655	356	130
Y	24	24	24	24	24	23	24	24	30
Zr	100	113	100	101	127	104	118	112	99
Ba	80	175	255	214	126	146	125	165	14
Pb	11	15	11	9	14	8	9	11	
Zn	110	132	123	98	129	80	68	109	
Cu	58	40	10	58	11	7	31	31	
Li	n.d.	70	52	49	68	56	49	59	

* total iron   ** without samples 6 and 7

In the SiO_2 versus (Na_2O + K_2O) diagram (fig. 6a) the samples plot in the tholeiitic field using the dividing line of IRVINE & BARAGAR (1971); they group close to the dividing line proposed by MacDONALD & KATSURA (1964). Here, however, we have to consider higher contents in alkalis due to secondary processes (see above) and SiO_2 losses of samples 1, 2 and 5.

The diagrams after FLOYD & WINCHESTER (1975), using the largely immobile elements, Ti, P, and Zr (fig. 6c, d) clearly show the tholeiitic character of the rock. The same is true for the SiO_2 versus Zr/TiO_2 diagram after FLOYD & WINCHESTER (1978) taking into consideration the SiO_2 losses of sample 1, 2 and 5 (fig. 6b).
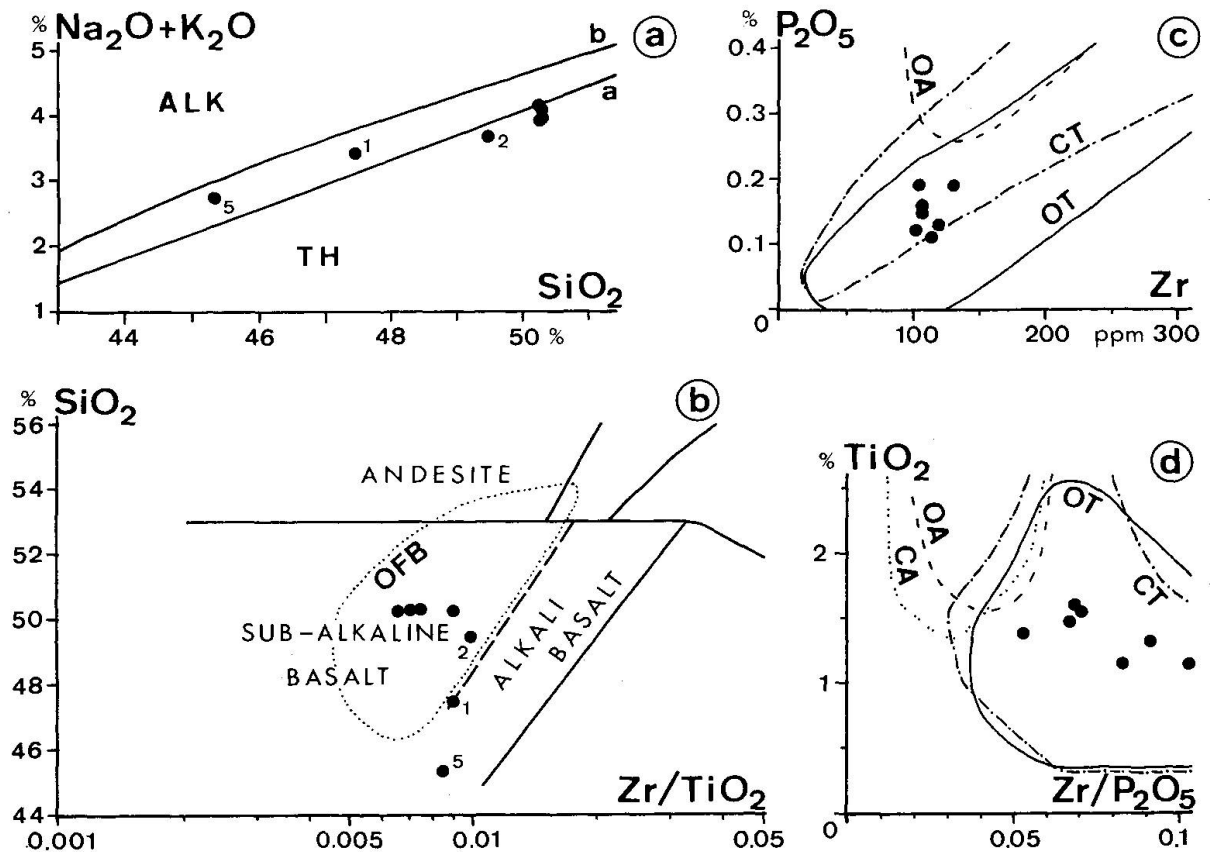
Fig. 6 6a. Diagram for the distinction between alkaline and tholeiitic series. a, dividing line after MacDonald & Katsura (1964), b, after Irvine & Baragar (1971). 6b: Diagram after Floyd & Winchester (1978). OFB, field of modern ocean-floor meta-basalts. 6c, d: Diagrams after Floyd & Winchester (1975). OA, CA, oceanic and continental alkaline basalts. OT, CT, oceanic and continental tholeiites.

In a number of diagrams after Miyashiro & Shido (1975) developed for sub-alkaline series and using the FeO_{tot}/MgO-ratio as a fractional differentation index, the samples plot in the fields of abyssal tholeiites (ocean-floor basalts) (fig. 7). It has to be emphasized that other tholeiitic basalts and calc-alkaline basalts may also plot in these fields as well as outside. In the Ni diagram this element shows irregular concentrations. Three samples (3, 6, 7) show markedly lower values and probably lost a good portion of their Ni during metamorphism.

Pearce & Cann (1973), Pearce et al., (1975), and Pearce (1975) developed a series of diagrams as a tool for a more detailed discrimination of basalts, especially the subalkaline series (fig. 8). In most diagrams the samples plot in the ocean-floor basalt fields.

In the diagram using Ti, Zr, and Y (fig. 8c), however, the samples group close to the border of the within-plate field. Considering the absolute values of element concentration (table 4), it is seen that TiO_2 and Zr correspond well with ocean-floor basalts but not with oceanic or continental within-plate basalts.
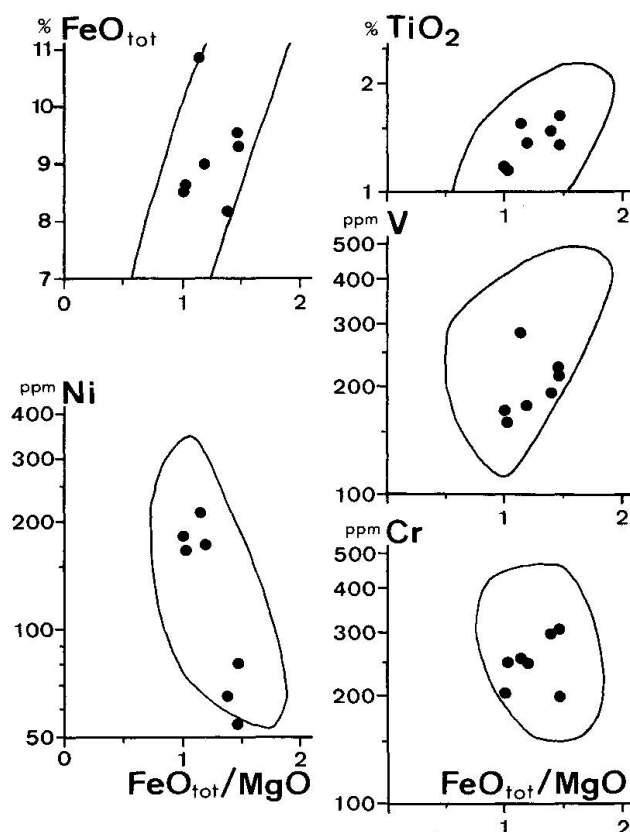
Fig. 7   Diagrams after MIYASHIRO & SHIDO (1975). Shown are the fields of abyssal tholeiites.

The Y-values better correlate with calc-alkaline basalts but, again, not with within-plate basalts.

Fig. 8e shows that the particularly mobile Sr migrated into most of the samples. In the TiO_2-K_2O-P_2O_2 triangle (fig. 8a) the two samples enriched in K_2O scatter but remain unchanged in their TiO_2/P_2O_5-ratio.

In another, recently published diagram using Ti, Mn, and P (MULLEN, 1983; fig. 9), all samples plot well within the ocean-floor basalt field.

Additional measurement on Nb (not listed in table 3) gives low values: 8, 13, 6, 10, 10, 12 and <5 ppm for samples 1 to 7, respectively. This confirms the non-alkaline tholeiitic character of the rock (Zr/TiO_2-Nb/Y and Zr/P_2O_5-Nb/Y diagrams in FLOYD & WINCHESTER, 1975, 1978).

The three-dimesional diagram of fig. 10 after PEARCE (1976) is based on the major elements and thus is problematic in being applied to metamorphosed rocks. Nevertheless, the samples generally group within the ocean-floor basalt field, and this may be an indication that changes in element concentration were not too large. The samples are again calculated with 1 % H_2O content. The effect
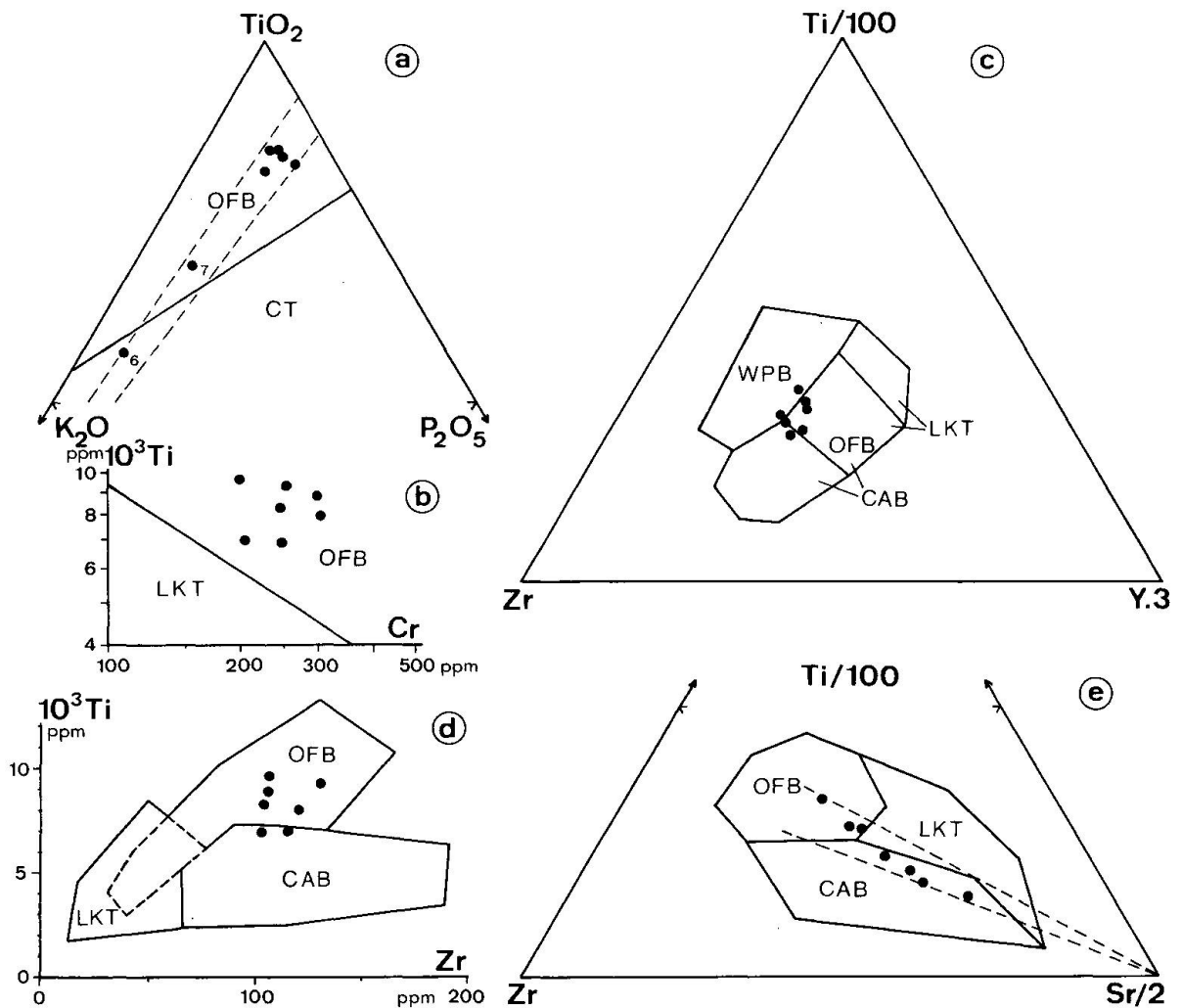
Fig. 8 Diagrams after PEARCE et al. (1975) (8a), PEARCE (1975) (8b) and PEARCE & CANN (1973) (8c–e) for the discrimination of basalts. OFB, ocean-floor basalts. CT, continental tholeiites. LKT, low-K (island-arc) tholeiites. CAB, calc-alkaline basalts. WPB, within-plate basalts.

of spilitization is shown by an arrow outside the diagram. The arrow points in the direction of the original composition with more CaO and less Na_2O. The K_2O-rich samples, especially sample 6, show a marked deviation towards shoshonite. The broken lines in the diagrams indicate the position when calculated with K_2O = 0,10% which is the mean of the other samples.

5. Discussion

The investigated epidote-amphibolite in the Kaserer Formation of the northwestern corner of the Tauern Window largely has the chemical characteristics of an ocean-floor basalt (MORB) which is slightly spilitized and partly contam-
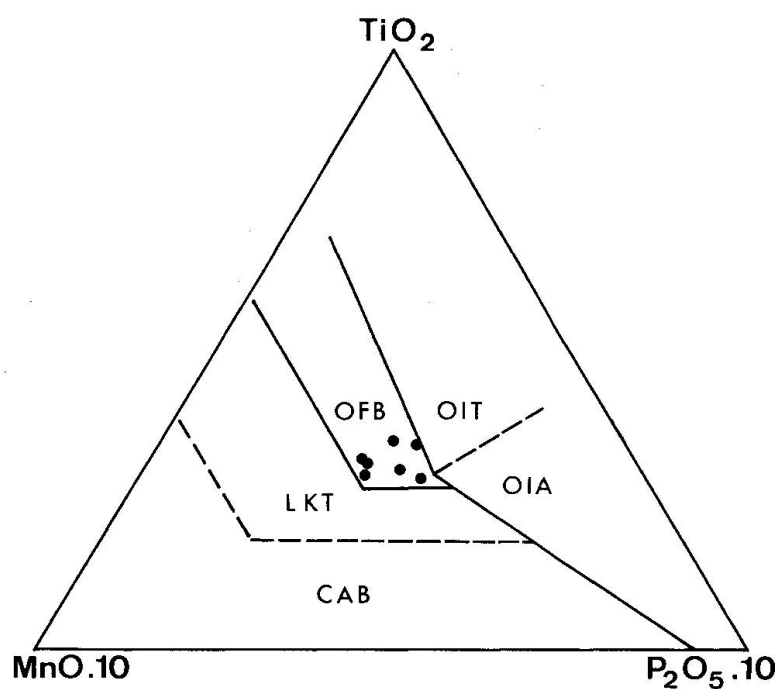
Fig. 9 Diagram after MULLEN (1983) for the discrimination of oceanic basalts. Abbreviations as in fig. 8. OIT, ocean island tholeiites. OIA, ocean island alkali basalts.
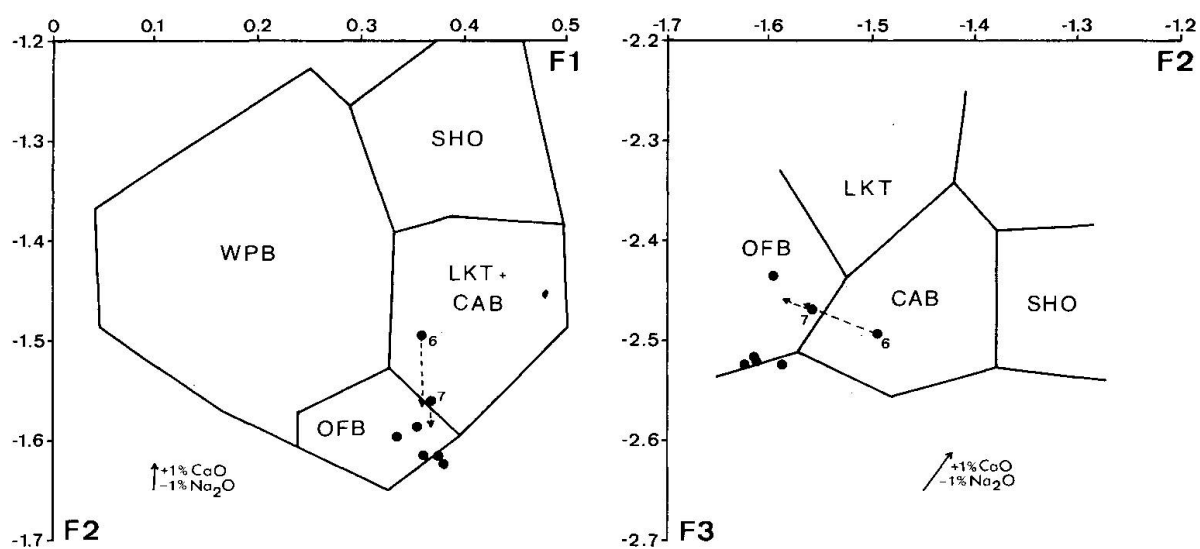

Fig. 10 Diagram after PEARCE (1976) using main element concentrations for the discrimination of basalts. Abbreviations as in fig. 8. SHO, shoshonite.

inated with potassium. On the other hand, continental tholeiites may have similar element concentrations als MOR basalts. This is of interest, as the northern continental slope of the South Penninic basin, on which the formation has been deposited, was already away from a mid-ocean environment in the Cretaceous. It may be argued, however, that the South Penninic ocean was a small and narrow basin. Thinned crust and active fault scarps would have created a possible environment for the ascent of tholeiitic basalts. Greenstones from the northern marginal part of the Bündner Schiefer of the Glockner nappe in the eastern part of the window gave results consistent with within–plate basalts, whereas greenstones in a central position of the Bündner Schiefer are of MOR origin (BICKLE & PEARCE, 1975).

The metamorphic history of the rock is complex. Relict amphibole points to an early phase of metamorphism with a higher P/T-ratio than the later low-grade regional metamorphism. This low-grade metamorphism was prograde. P is estimated to about 4 kb at 500°C but this value remains uncertain. T increased towards the S(W) and reached more than 500°C but remained within the low-grade range.

The relict amphibole may be correlated with the early Alpidic metamorphism known from the base of the Glockner nappe in the southern parts of the western and central Tauern Window. There, this metamorphism is of high-P/T character, and is attributed to subduction in the Cretaceous. The Kaserer Formation may have been involved in this process at the time the Middle Penninic Venediger nappe collided and was thrust under the nappe pile in the south (FRISCH, 1978). Underthrusting was certainly not too far-reaching for the Middle Penninic microcontinent, but at least its marginal parts suffered some metamorphism with a probably higher P/T-ratio as during the Lower Tertiary metamorphic event. This is also indicated by a finding of lawsonite pseudomorphs from the Felbertauern road tunnel in the basement of the Venediger nappe. Rhomb-shaped pseudomorphs mainly composed of epidote were described from a hornblendite by FRISCH (1970). In the Bündner Schiefer of the Glockner nappe similar occurrences were interpreted by FRY (1973) as replaced lawsonites. The real age of this lawsonite is, of course, not known.

Regional metamorphism with its climax towards the end of the Eocene has obliterated nearly all the traces of the Cretaceous event. The overburden was less than during the Cretaceous event.

References

BICKLE, M.J. & PEARCE, J.A. (1975): Oceanic mafic rocks in the Eastern Alps. Contrib. Mineral. Petrol., 49, 177–189.

BLESER, P. (1934): Geologische Studien am Westende der Hohen Trauern östlich der Brennerlinie. Bull. Inst. Grand-Ducal Luxembourg, Archives, n.s., 13, 89pp., Luxembourg.

BROWN, E.H. (1977): The crossite content of Ca-amphibole as a guide to pressure of metamorphism. J. Petrol., 18, 53–72.

ENGEL, A.E.J., ENGEL, C.G. & HAVENS, R.G. (1965): Chemical characteristics of oceanic basalts and the upper mantle. Geol. Soc. Amer. Bull., 76, 719–734.

FLOYD, P.A. & WINCHESTER, J.A. (1975): Magma type and tectonic setting discrimination using immobile elements. Earth Planet. Sci. Lett., 27, 211–218.

FLOYD, P.A. & WINCHESTER, J.A. (1978): Identification and discrimination of altered and metamorphosed volcanic rocks using immobile elements. Chem. Geol., 21, 291–306.

FRISCH, W. (1968): Zur Geologie des Gebietes zwischen Tuxbach und Tuxer Hauptkamm bei Lanersbach (Zillertal, Tirol). Mitt. Ges. Geol. Bergbaustud. Wien, 18, 287–336.

FRISCH, W. (1970): Geologie und Petrographie des Felbertauern-Strassentunnels (Osttirol). N. Jb. Geol. Paläont. Abh. 134, 267–282.

FRISCH, W. (1978): A plate tectonics model of the Eastern Alps. In: CLOSS, H., ROEDER, D. & SCHMIDT, K. (eds.), Alps, Apennines, Hellenides, p. 167–172, Stuttgart (Schweizerbart).

FRISCH, W. (1980): Post-Hercynian formations of the western Tauern window: Sedimentological features, depositional environment, and age. Mitt. Österr. Geol. Ges., 71/72, 49–63.

FRY, N. (1973): Lawsonite pseudomorphed in Tauern greenschist. Min. Mag., 39, 121–122.

HART, R.A. (1976): Chemical variance in deep ocean basalts. Initial Rep. DSDP, 34, 301–335.

HIETANEN, A. (1974): Amphibole pairs, epidote minerals, chlorite, and plagioclase in metamorphic rocks, northern Sierra Nevada, California. Amer. Min., 59, 22–40.

HÖCK, V. (1969): Zur Geologie des Gebietes zwischen Tuxer Joch und Olperer (Zillertal, Tirol). Jb. Geol. B. A. Wien, 112, 163–195.

HOERNES, S. & FRIEDRICHSEN, H. (1974): Oxygen isotope studies on metamorphic rocks of the Western Hohe Tauern area (Austria). Schweiz. Min. Petr. Mitt., 54, 769–788.

HOSCHEK, G. (1980): Phase relations of a simplified marly rock system with application to the Western Hohe Tauern (Austria). Contrib. Mineral. Petrol., 73, 53–68.

IRVINE, T.N. & BARAGAR, W.R.A. (1971): A guide to the chemical classification of the common volcanic rocks. Canad. J. Earth. Sci., 8, 523–548.

LAIRD, J. (1982): Amphiboles in metamorphosed basaltic rocks: greenschist facies to amphibolite facies. – In: VEBLEN, D.R. & RIBBE, P.H. (eds.), Amphiboles: petrology and experimental phase relations. Reviews in Mineralogy, 9B, 390pp., Min. Soc. Amer., Washington D.C.

LAIRD, J. & ALBEE, A.L. (1981): Pressure, temperature, and time indicators in mafic schist: their application to reconstructing the polymetamorphic history of Vermont. Amer. J. Sci., 281, 127–175.

LEAKE, B.E. (1965): The relationship between tetrahedral aluminium and the maximum possible octahedral aluminium in natural calciferous and subcalciferous amphiboles. Amer. Mineralogist, 50, 843–851.

LEAKE, B.E. (1971): On aluminous and edenitic hornblendes. Miner. Mag., 38, 389–407.

MACDONALD, G.A. & KATSURA, T. (1964): Chemical composition of Hawaiian lavas. J. Petrol., 5, 82–133.

MIYASHIRO, A. & SHIDO, F. (1975): Tholeiitic and calc-alkalic series in relation to the behaviour of titanium, vanadium, chromium, and nickel. Amer. J. Sci., 275, 265–277.

MULLEN, E.D. (1983): $MnO/TiO_2/P_2O_5$: a minor element discriminant for basaltic rocks of oceanic environments and its implications for petrogenesis. Earth Planet. Sci. Lett., 62, 53–62.

PEARCE, J.A. (1975): Basalt geochemistry used to investigate past tectonic environments on Cyprus. Tectonophysics, 25, 41–67.

PEARCE, J.A. (1976): Statistical analysis of major element patterns in basalts. J. Petrol., 17, 15–43.

PEARCE, J.A. & CANN, J.R. (1973): Tectonic setting of basic volcanic rocks determined using trace element analyses. Earth Planet. Sci. Lett., 19, 290–300.

PEARCE, T.H., GORMANN, B.E. & BIRKETT, T.C. (1975): The TiO_2-K_2O-P_2O_5 diagram: a method of discriminating between oceanic and non-oceanic basalts. Earth Planet. Sci. Lett., 24, 419–426.

RAASE, P. (1974): Al and Ti contents of hornblende, indicators of pressure and temperature of regional metamorphism. Contrib. Mineral. Petrol., 45, 231–236.

RAITH, M. (1976): The Al-Fe(III) epidote miscibility gap in a metamorphic profile through the Penninic series of the Tauern Window, Austria. Contrib. Mineral. Petrol., 57, 99–117.

SANDER, B. (1911): Geologische Studien am Westende der Hohen Tauern (Erster Bericht). Denkschr. Adad. Wiss. Wien, math.-nat. Kl., 82, 257–319.

THIELE, O. (1970): Zur Stratigraphie und Tektonik der Schieferhülle der westlichen Hohen Tauern. Verh. Geol. B. A., 1970, 230–244.

VOLL, G. (1980): Ein Querprofil durch die Schweizer Alpen vom Vierwaldstättersee zur Wurzelzone – Strukturen und ihre Entwicklung durch Deformationsmechanismen wichtiger Minerale. N. Jb. Geol. Paläont. Ab., 160, 321–335.

WINKLER, H.G.F. (1979): Petrogenesis of metamorphic rocks. 5th ed., 348 pp., Springer-Verlag, New York–Heidelberg–Berlin.